

# Improved ovarian cancer EMT-CTC isolation by immunomagnetic targeting of epithelial EpCAM and mesenchymal N-cadherin

Joseph W Po<sup>1,2</sup>, Aflah Roohullah<sup>1,2,3</sup>, David Lynch<sup>1,2</sup>, Anna DeFazio<sup>4,5,6</sup>, Michelle Harrison<sup>3,7</sup>, Paul R Harnett<sup>4,5,6</sup>, Catherine Kennedy<sup>4,5,6</sup>, Paul de Souza<sup>1,2,3,8</sup>, and Therese M Becker<sup>1,2,4,8</sup>

## Abstract

Epithelial cell adhesion molecule (EpCAM)-targeted capture remains the most common isolation strategy for circulating tumor cells (CTCs). However, epithelial-to-mesenchymal transition (EMT) leads to decreased epithelial EpCAM expression affecting the optimal CTC capture. In this study, we tested a cohort of ovarian cancer cell lines using flow cytometry to identify N-cadherin as the additional immunomagnetic cell surface target for ovarian cancer cell isolation. Combined immunomagnetic targeting of mesenchymal N-cadherin and epithelial EpCAM enriched CTCs from advanced ovarian cancer patient blood approximately three times more efficiently than targeting of EpCAM alone. We also show that more EMT-phenotype CTCs are captured by including N-cadherin targeting into CTC isolation protocols. However, after N-cadherin-based CTC isolation, in some blood samples of healthy individuals, we also observed the presence of cells expressing markers common to CTCs. Our data show that these “false positives” can be largely distinguished from CTCs as circulating endothelial cells (CECs) by vascular endothelial–cadherin co-staining. CEC counts are highly variable in patients and healthy controls. Our data demonstrate that a combination of EpCAM with N-cadherin-targeted isolation can improve CTC detection and widen the EMT-phenotype spectrum of captured CTCs.

## Keywords

CTC, EMT, EpCAM, N-cadherin, VE-cadherin, vimentin

Date received: 1 January 2018; accepted: 11 April 2018

<sup>1</sup> Centre for Circulating Tumour Cell Diagnostics and Research, Ingham Institute for Applied Medical Research, Liverpool, New South Wales, Australia

<sup>2</sup> School of Medicine, Western Sydney University, Campbelltown, New South Wales, Australia

<sup>3</sup> Department of Medical Oncology, Liverpool Hospital, Liverpool, New South Wales, Australia

<sup>4</sup> Centre for Cancer Research, Westmead Institute for Medical Research, Westmead, New South Wales, Australia

<sup>5</sup> The University of Sydney, New South Wales, Australia

<sup>6</sup> The Crown Princess Mary Cancer Centre Westmead, Westmead Hospital, New South Wales, Australia

<sup>7</sup> Department of Medical Oncology, Chris O'Brien Lifehouse, Camperdown, New South Wales, Australia

<sup>8</sup> South Western Clinical School, University of New South Wales, Liverpool, New South Wales, Australia

## Corresponding Author:

Therese Becker, Ingham Institute for Applied Medical Research, 1 Campbell St., Liverpool, New South Wales 2170, Australia.

Email: t.becker@unsw.edu.au



## Introduction

Ovarian cancer is the fifth leading cause of cancer in women and the leading cause of gynecological cancer death worldwide. While 70–80% of patients initially respond to first-line platinum-based chemotherapy, others have intrinsically resistant tumors. Further, the majority (70%) of advanced-stage patients will eventually develop treatment resistance.<sup>1,2</sup>

The analysis of circulating tumor cells (CTCs) is emerging as a promising way to monitor cancer progression and the effectiveness of therapy. CTCs are cells that have shed from the primary or metastatic tumor and intravasated into the blood stream. CTC isolation and analysis can give an insight into the disease biology and its behavior. Expectedly, high CTC counts have been correlated with disease progression and poorer prognosis in colorectal, breast, and prostate cancers (reviewed by Caixeiro et al.<sup>3</sup>). A comprehensive study in ovarian cancer patients ( $n = 216$ ) showed that CTC counts above two at therapy commencement correlated with poorer progression-free and overall survival.<sup>4</sup> Another study found that enhanced CTC counts predicted relapse or progression in 31 epithelial ovarian cancer patients.<sup>5</sup> Although some smaller studies found no correlation of CTCs with disease progression, four recent meta-analyses showed that CTC positivity in ovarian cancer patients was significantly associated with shorter overall, disease-free, and progression-free survival as well as advanced stage in ovarian cancer.<sup>6–9</sup>

Potential diagnostic application of ovarian cancer patient CTCs include CTC ERCC1 transcript detection associated with platinum resistance, detection of CTC clusters associated with platinum resistance, and in vitro assaying of platinum sensitivity in cultured CTCs which correlated with patient response.<sup>10–12</sup> Thus, although CTCs are often considered of minor relevance in ovarian cancer because it metastasizes mainly throughout the peritoneum, a view that was challenged by data using an elegant parabiosis mouse model, ovarian cancer CTCs appear to have value as biomarkers.<sup>13,14</sup>

Currently, the most common method of CTC isolation relies on immunomagnetic cell capture by targeting the epithelial cell adhesion molecule (EpCAM). However, with EpCAM expression lost or reduced, CTC detection may be difficult,<sup>15,16</sup> and there is evidence for EpCAM heterogeneity in ovarian cancer cells.<sup>17</sup> Moreover, EpCAM is downregulated during epithelial-to-mesenchymal transition (EMT), a process that is implicated in the metastatic spread of cancer and especially the egress of CTCs into the circulation.<sup>18</sup> A recent study evaluating epithelial and mesenchymal gene expression of ovarian cancer patient CTCs before and after chemotherapy suggested that platinum-based therapy enriches EMT-like CTCs.<sup>19</sup> Similarly, EMT-phenotype changes may be a marker of resistance to platinum therapy as shown for ovarian cancer cell lines,<sup>20</sup> and gradual change towards EMT gene expression

signatures in ovarian cancer tissue during progression to platinum resistance was correlated with poor prognosis.<sup>21,22</sup> Quite contrary, another study indicates that the epithelial cell phenotype combined with high nuclear factor  $\kappa$ B activity is associated with ovarian cancer platinum resistance.<sup>23</sup> Taking the evidence together, liquid biopsies and CTC analysis may provide important predictive and prognostic information, and heterogeneity in resistance mechanisms suggest that both epithelial and mesenchymal cells need to be investigated to follow changes of disease progression biomarkers in a representative population of CTCs.

A well-characterized central step during EMT is the expression switch of the epithelial cell–cell adhesion molecule E-cadherin to the mesenchymal cell–cell adhesion molecule N-cadherin (reviewed by Lamouille et al.<sup>24</sup>), and an E-cadherin-to-N-cadherin switch was shown in ovarian cancer tissue at progression from stage II to stage III.<sup>25</sup> Therefore, in this study, we assessed E-cadherin, EpCAM, and N-cadherin expression on the surface of ovarian cancer cell lines to identify N-cadherin, in addition to EpCAM, as a useful target for immunomagnetic CTC isolation. We demonstrate that additional CTCs are isolated by combining EpCAM with N-cadherin-targeted CTC isolation by establishing a method to identify EMT-phenotype CTCs.

## Materials and methods

### Patients

Patients were recruited from Liverpool Cancer Therapy Centre and The Crown Princess Mary Cancer Centre Westmead. Clinical information was sourced from patient medical records. Information at the time of blood sampling was collected including age and primary cancer site. Treatment information was collected including chemotherapy regimen, previous lines of therapy prior to CTC isolation, serum CA-125 levels, and radiological assessments (Online Supplementary Table S1). Blood samples from healthy individuals were analyzed as controls.

### Cell culture

Ovarian cancer cell lines A2780, CAOV3, COLO316, ES2, OVCAR3, PEO1, PEO4, PEO14, SKOV3, and the WME-099 EBV-transformed human B-lymphocyte cell line were maintained in RPMI 1640 media (Lonza, Basel, Switzerland) supplemented with 10% fetal bovine serum (FBS) (Interpath, Melbourne, Australia) in a humidified incubator with 5% atmospheric carbon dioxide at 37°C. All cell lines were authenticated by Short Tandem Repeat (STR) Profiling (Australian Genome Research Facility, Melbourne, Australia) and tested negative for mycoplasma. Cells were seeded at 15–20% confluency and cultured for 3 days. Adhered cells were harvested with 0.2 mM ethylenediaminetetraacetic acid (EDTA) in phosphate-buffered saline

(PBS) at 37°C to maintain cell surface protein integrity. Cell scrapers were used to help detach any cell adhering beyond 5–10 min of PBS/EDTA incubation.

### Flow cytometry

Detached cells were pelleted, resuspended, and aliquoted at  $1-5 \times 10^5$  cells. Cells were blocked with 10% FBS in PBS and probed sequentially with primary and secondary antibodies for 30 and 20 min, respectively (Online Supplementary Table S2) and resuspended in 300 µl of PBS for fluorescence-activated cell sorting (FACS) analysis (FACS Canto II Cell Analyzer, BD Biosciences, North Ryde, Australia). Flowing Software 2.5.1 was used for analysis (Turku Centre for Biotechnology, Turku, Finland).

### Immunocytochemistry

Cells were seeded on sterile 18-mm diameter coverslips in 12-well plates at  $2.5 \times 10^4$  cells/well and grown for 3 days. Non-fixed cells were blocked with 10% FBS in PBS for 10 min and sequentially incubated with primary and secondary antibodies for 45 and 30 min, respectively (Online Supplementary Table S2). ProLong Gold Antifade reagent with 4',6-diamidino-2-phenylindole (DAPI) (Life Technologies, Melbourne, Australia) was used for mounting. Fluorescent microscopy cell images were taken with a BX53 microscope (Olympus, Notting Hill, Australia) with 20× objective using the CellSens Dimension imaging software.

### CTC capture

Immunomagnetic beads, Rare Cell Isolation Kit (Fluxion, San Francisco, California, USA), were incubated with anti-EpCAM or anti-N-cadherin antibodies for conjugation according to the distributor's protocol (Online Supplementary Table S2). Conjugated beads were stored at 4°C and used within 4 weeks.

At each blood collection, three 9 ml peripheral blood tubes were drawn per patient into EDTA vacutubes (Greiner Bio-One, Frickenhausen, Germany) and processed within 24 h. A total of 26 blood collections from 22 patients were analyzed.

Lymphoprep and Sepmate tubes (Stemcell Technologies, Vancouver, Canada) were used to separate the peripheral blood mononuclear cells (PBMCs), containing CTCs, according to the manufacturer's instructions. PBMCs derived from 9 ml blood each were washed once in PBS and resuspended in 800 µl binding buffer; then, 40 µl FC buffer (Fluxion) and either 30 µl anti-EpCAM antibody-coupled beads or 30 µl anti-N-cadherin antibody-coupled beads or 30 µl of each were added. Cells were incubated for 90 min at 4°C on a rotating platform and then loaded into primed IsoFlux cartridges for CTC enrichment using the IsoFlux standard isolation protocol (Fluxion). Enriched

CTCs samples were fixed with 3.7% formaldehyde in PBS before immunocytochemistry.

### CTC immunocytochemistry

Enriched CTC samples were washed with binding buffer and blocked with 25 µl of 10% FBS in binding buffer, followed by 15-min incubation with 25 µl of anti-CD45 antibody (Fluxion), 1:100 in 10% FBS/binding buffer. After a binding buffer wash, cells were incubated with 25 µl Cy3-conjugated donkey anti-rabbit immunoglobulin G (IgG) antibody (Fluxion), 1:200 dilution in 10% fetal calf serum (FCS)/binding buffer for 15 min, washed again, then permeabilized with 25 µl 0.2% Triton X-100, and incubated with 25 µl of fluorescein isothiocyanate (FITC) conjugated anti-cytokeratin antibody diluted in 10% FCS/binding buffer (Online Supplementary Table S2) for 30 min. After final wash steps, samples were transferred to glass slides and mounted with ProLong Gold Antifade reagent with DAPI (Life Technologies, Melbourne, Australia). Cells were imaged as outlined above. Initially, CTCs from the blood samples of 10 patients and 10 healthy blood donors were detected and enumerated in this standard way by establishing nuclear DAPI (Nuc+), cytokeratin (CK+), and CD45- cells.

### VE-cadherin quadruple immunocytochemistry

For quadruple staining, enriched CTC samples were pre-blocked with mouse immunoglobulins as above. After fixing in 3.7% formaldehyde, the CTC immunocytochemistry protocol was followed by the Cy3-conjugated donkey anti-rabbit IgG antibody probing. Sample was then washed in binding buffer and incubated with VioBlue-conjugated antihuman vascular endothelial (VE)-cadherin (cad) antibody for 30 min (Online Supplementary Table S2), followed by cytokeratin probing. Sample mounting media included DRAQ5 nuclear dye (Abcam, Melbourne, Australia) instead of DAPI. Imaging was performed as outlined above. VioBlue VE-cad staining was scored immediately in Nuc+/CK+/CD45- cells to avoid background associated with slide storage. Blood samples from six patients and nine healthy donors were analyzed this way.

Finally, blood samples from six patients were compared using quadruple staining with either antihuman vimentin or VE-cad antibodies (as described above) analyzing CTC isolations based on targeting either the cell surface marker EpCAM or the combination of EpCAM and N-cadherin.

### Vimentin quadruple immunocytochemistry

For quadruple CTC and vimentin staining, enriched CTC samples were preblocked in 25 µl mouse immunoglobulins (Abacus, Brisbane, Australia) at a final concentration of 1.2 µg/µl in binding buffer for 20 min to saturate any

remaining free anti-mouse antibody present on magnetic beads. Samples were then washed briefly in binding buffer and fixed in 3.7% formaldehyde for 10 min. Initially, the CTC immunocytostaining protocol was followed. After the cytokeratin probing, samples were washed in binding buffer and incubated with Alexa Fluor 647-conjugated mouse antihuman vimentin antibody for 1 h at room temperature (Online Supplementary Table S2). After three washes ( $2 \times$  PBS,  $1 \times$  H<sub>2</sub>O) mounting media included Hoechst nuclear dye, and cells were observed and images were captured as mentioned earlier. Nuc+/CK+/CD45– cells were scored as EMT-CTCs when showing strong vimentin reactivity (Vim+).

### *N-cadherin quadruple immunocytostaining*

For N-cadherin quadruple CTC staining, enriched CTC samples or PBMCs were preblocked with mouse immunoglobulins and then washed, fixed, and blocked as mentioned earlier. Samples were then incubated with FITC-conjugated anti-CD45 (Biolegend, San Diego, CA, USA) and FITC-conjugated anti-CD144 (Miltenyi Biotec, NSW, Australia) for 30 min. Samples were washed in binding buffer and probed with rabbit anti-N-cadherin (Novus, Biologicals, Littleton CO, USA) for 60 min and then its AlexaFluor647-conjugated secondary donkey anti-rabbit IgG antibody (Jackson ImmunoResearch, West Grove, PA, USA) for 30 min. After permeabilization with 0.2% Triton-X in PBS, samples were probed with AlexaFluor555-conjugated pan-cytokeratin (Cell Signaling Technology, Beverly, MA, USA) for 30 min (see Online Supplementary Table S2, for antibody dilutions). After three washes ( $2 \times$  PBS,  $1 \times$  H<sub>2</sub>O), cells were observed and images captured as mentioned earlier.

### *Compliance with ethical research standards*

The study was conducted in accordance with the Declaration of Helsinki and approved by the South Western Sydney Local Health District Ethics Committee (Ref: HREC/13/LPOOL/158). All patients and healthy controls included in this study gave informed written consent for blood collection and subsequent CTC analysis.

## **Results**

### *Epithelial and mesenchymal cell surface proteins on ovarian cancer cells*

To identify suitable ovarian cancer cell surface proteins for evaluating immunomagnetic CTC isolation, a heterogeneity representative cohort of nine different ovarian cancer cell lines was analyzed by FACS and immunocytostaining for the expression of E-cadherin, EpCAM, and N-cadherin. A human B-lymphocyte cell line (WME-099) was included in the analysis to rule out antibody interaction with lymphocytes. As expected, EpCAM was heterogeneously

expressed and was never found on the entire cell population of any ovarian cancer cell line. In all, 60–85% of cells expressed detectable EpCAM levels, while in two cell lines, ES-2 and A2780, EpCAM was undetectable. E-cadherin expression was found in the same cell lines that expressed EpCAM, although the proportion of cells expressing detectable E-cadherin tended to be slightly lower, ranging from 30% to 80%, again ES-2 and A2780 lacked E-cadherin. N-cadherin expression, on the other hand, tended to be inversely related to EpCAM expression, with EpCAM-negative ES-2 cells expressing detectable N-cadherin in approximately 80% of cells. Exceptions were EpCAM and E-cadherin-positive PEO14 cells that also expressed high N-cadherin levels in approximately 75% of cells, while EpCAM/E-cadherin-negative A2780 cells also lacked detectable N-cadherin in the majority (>60%) of cells (Figure 1). Overall, N-cadherin emerged as a possible target for EMT-CTC isolation.

### *N-cadherin-targeted CTC isolation from advanced ovarian cancer patients*

CTC isolation was performed using the Isoflux microfluidic CTC isolation instrument. We confirmed in initial experiments that the GC-4 anti-N-cadherin antibody is suitable for immunomagnetic cell capture of ES-2 cells (data not shown). To validate that N-cadherin in addition to EpCAM targeting improves CTC isolation, we compared CTC isolation in 20-patient blood collections from 18 advanced ovarian cancer patients when analyzed according to standard CTC identification (Nuc+/CK+/CD45–). CTCs were captured in 90% (18 of 20) of the patient samples when EpCAM and N-cadherin were targeted together, and slightly fewer (80%, 16 of 20) by directing isolation at EpCAM alone (Figure 2(a), Table 1). CTC counts showed high intra-patient variability in all antibody groups (0–376 for EpCAM–, 0–853 for N-cadherin–, and 0–1300 for combined targeted isolation). N-cadherin-directed CTC isolation outperformed EpCAM-based isolation by 2.1-fold, based on median fold change of CTC capture, while combined targeting of N-cadherin and EpCAM increased CTC capture 3.0-fold (Table 1). In 10 healthy blood donor control samples, we also observed a background of cells that met the staining criteria for CTCs when N-cadherin alone or in combination with EpCAM was targeted for isolation. Importantly, these “false-positive CTCs” were highly variable in number, and most healthy individuals had only moderate counts. However, 40% (4 of 10) of healthy individuals had >10 cells in 9 ml blood meeting the CTC definition of Nuc+/CK+/CD45– (Figure 2(b)).

### *Distinguishing CECs from CTCs*

Circulating endothelial cells (CECs) are rare cells in the circulation, expressing N-cadherin and cytokeratin<sup>28</sup> and thus are likely to be co-enriched with our assay as “false-

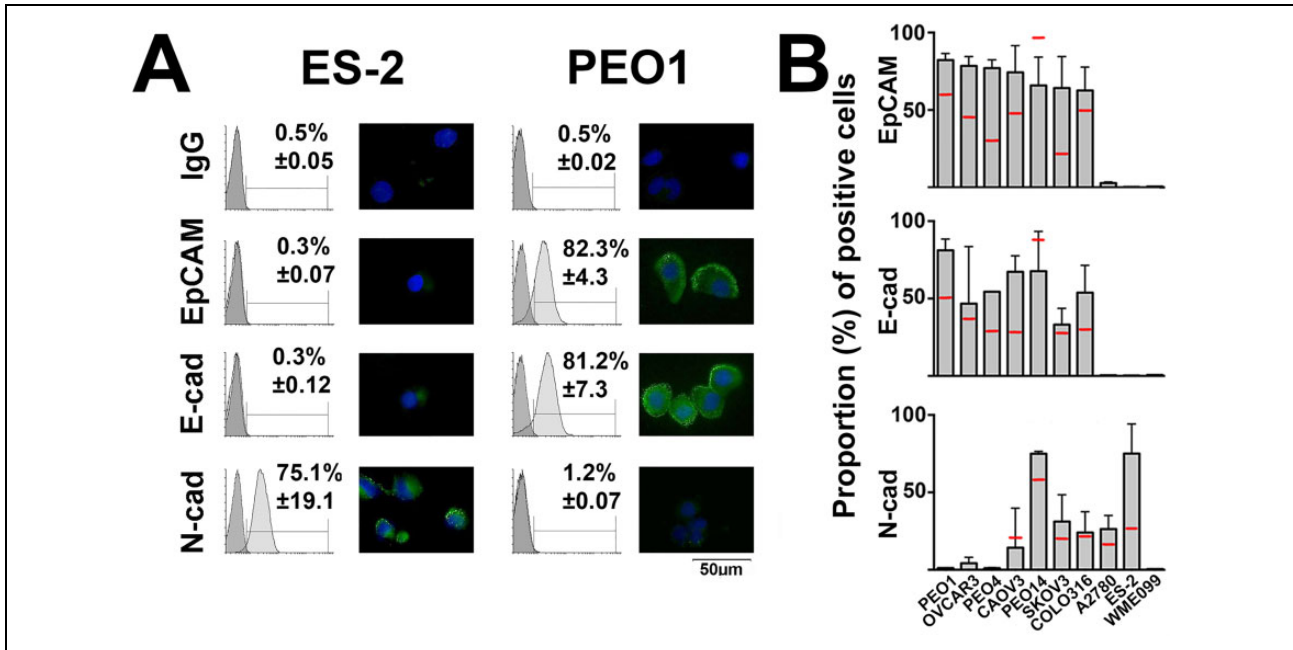


**Figure 1.** Cell surface proteins on ovarian cancer cells and lymphocytes. The nine indicated ovarian cancer cell lines and the lymphocyte line WMM-099 were tested for the expression of EpCAM, E-cadherin (E-cad), and N-cadherin (N-cad) by FACS analysis and immunocytochemistry. (a) Representative FACS histograms and immunocytochemistry for mesenchymal ES-2<sup>26</sup> and epithelial PEO1 cells<sup>27</sup> are depicted. (b) The proportion (gray columns) of cells from the indicated cell lines expressing the designated proteins with mean expression level (red bars) is graphed (mean  $\pm$  SEM,  $n \geq 2$ ). FACS: fluorescence-activated cell sorting; SEM: standard error of mean.

**Table 1.** Comparative CTC isolation approaches with indicated antibodies presented by common CTC identification (Nuc+/CK+/CD45-).

Patient	EpCAM	N-cadherin	Fold change	Combination	Fold change
Pt 1	20	38	1.9	24	1.2
Pt 2	0	17	—	2	—
Pt 3	0	0	—	0	—
Pt 4	19	25	1.3	58	3.1
Pt 5*	8	288	36.0	82	10.3
Pt 6	48	82	1.7	125	2.6
Pt 7	376	853	2.3	1300	3.5
Pt 7 <sup>a,*</sup>	236	307	1.3	697	3.0
Pt 8	8	24	3.0	42	5.3
Pt 9*	16	162	10.1	68	4.3
Pt 10	4	7	1.8	9	2.3
Pt 11	0	0	—	0	—
Pt 12	51	530	10.4	465	9.1
Pt 13	7	47	6.7	29	4.1
Pt 13 <sup>a</sup>	20	38	1.9	74	3.7
Pt 14	6	46	7.7	8	1.3
Pt 15	0	2	—	1	—
Pt 16	5	21	4.2	8	1.6
Pt 17	4	6	1.5	9	2.3
Pt 18	4	3	0.8	1	0.3
	<b>Median fold change</b>		<b>2.1</b>	<b>Median fold change</b>	<b>3.0</b>

CTC counts per 9 ml blood. Data from 20 blood collections (18 patients) with CTCs stained by the common identification stain (Nuc+/CK+/CD45-) ( $n = 10$ ) or relevant data from common stain plus Vim ( $n = 4$ ) or VE-cadherin ( $n = 6$ ) are combined. Pt: patient; EpCAM: epithelial cell adhesion molecule; CTCs: circulating tumor cells.

<sup>a</sup>Recollection post >3 months.

\* <9ml blood available, data normalised to 9ml.

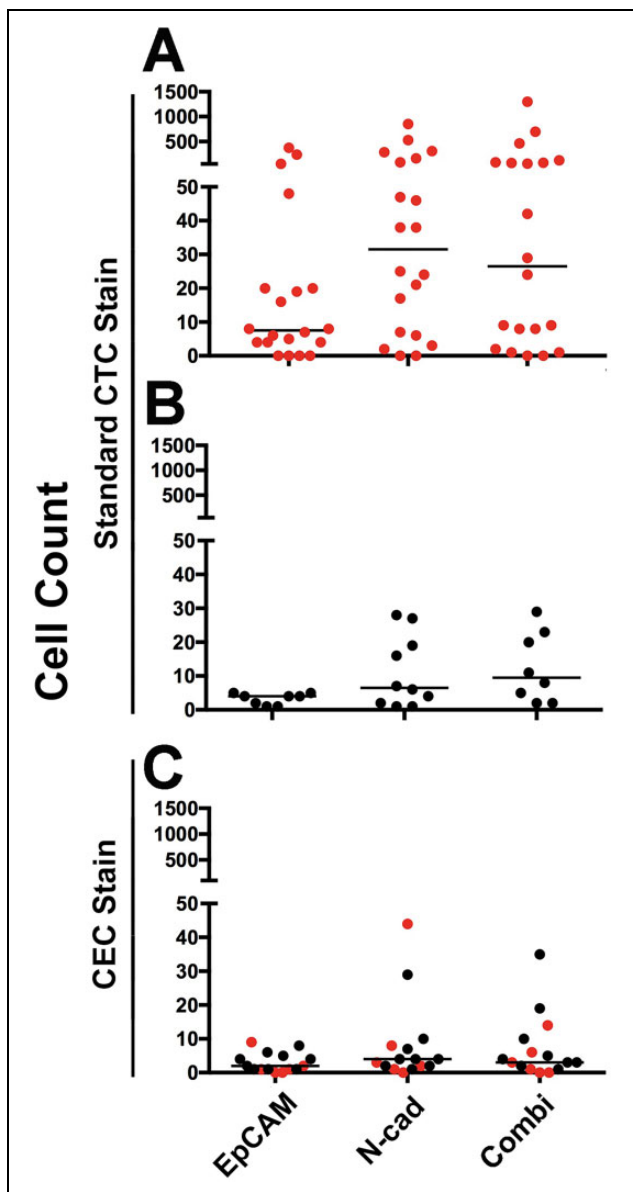


**Figure 2.** Cell isolation from advanced ovarian cancer patients. (a) Data from 20 blood collections (18 patients) are presented to compare EpCAM, N-cadherin (N-cad), or the combination (Combi) targeted CTC isolation efficiencies when applying the standard CTC identification (Nuc+, CK+, and CD45-). (b) False-positive “CTCs” in 10 healthy donor blood samples, when using the standard CTC identification (Nuc+, CK+, and CD45-). (c) CECs in healthy individuals and patients: the same cell isolation method using a VE-cadherin (VE-cad) CEC staining protocol identified co-isolated CECs in patients ( $n = 6$ ) and healthy controls ( $n = 9$ ). Red symbols: patient-derived CTCs (a) or CECs (c); black symbols: healthy control-derived false positive “CTCs” (b) or CECs (c). All counts are presented as cells per 9 ml blood. EpCAM: epithelial cell adhesion molecule; CTCs: circulating tumor cells; CECs: circulating endothelial cells.

positive CTCs” when isolation is directed at EMT markers. To identify CECs, a quadruple-staining identification strategy, including probing for the endothelial marker VE-cad, revealed that isolated CECs (Nuc+/CK+/VE-cad+/

CD45-) were enriched in blood collections from our patients and healthy controls with comparable distribution to the cells we identified as “false-positive CTCs” (Figure 2(b) and (c)). To help estimate how much of an issue false positive (non-CTCs) are for this assay, we spiked SKOV3 cells into healthy donor blood and compared a small proportion of pre-enrichment PBMCs with the major proportion of blood after CTC enrichment using the same staining. Mimicked CTCs (SKOV3) were found in the pre-enrichment sample, consistent with the minor proportion of PBMCs analyzed. Importantly, more cells met the CEC criteria in the pre-enriched sample (5 from 1 ml blood vs. 1 after N-cadherin-based CTC enrichment from 8.7 ml blood). Together with the fact that no CECs were detected after EpCAM or combined targeted CTC enrichment, this indicates that the healthy donor had relatively low overall CEC counts (Online Supplementary Figure S1).

The prevalence of CECs in ovarian cancer patients and healthy controls confirmed that CEC co-isolation by EpCAM targeting is rare, while N-cadherin targeting is associated with increased identification of co-isolated CECs. CEC counts are highly variable between individuals and low (<5) in approximately 60% of assayed healthy controls and patient samples. Strikingly though, in patient 14, CECs (44 of 46) outnumbered CTCs (2 of 46) (Figure 3(a)), highlighting the value of CEC co-staining during CTC identification.

#### EMT-CTC detection and discrimination from CECs

To confirm that we can detect EMT-CTCs, we developed another quadruple stain for Nuc+/CK+/CD45- CTCs by including the EMT marker vimentin (Vim) into our immunomagnetic CTC isolation method. Due to limitations of our microscope (four-color detection only), we were unable to include Vim and VE-cad detection in the same assay.

To determine whether contaminating CECs will affect EMT-CTC detection, we decided to focus on CTCs isolated by either EpCAM alone or in combination with N-cadherin targeting. We performed a quadruple stain for VE-cad or for Vim in CTCs of parallel samples from six patients, five positive for CTCs (Figure 3(b)). EMT-CTCs were observed at higher counts than CECs in the majority of patient samples regardless of isolation method. Only patient 22 displayed higher CEC counts than EMT-CTC counts associated with CTC isolation by combination targeting. Importantly, regardless of varying CEC co-purification, true EMT-CTC counts were always higher in combination-based CTC isolates in comparison to EpCAM-alone-based isolation (Figure 3(b)).

To estimate how prevalent rare blood cell expression of N-cadherin is and how well we are able to distinguish EMT-CTCs from potential false positives, we took 27ml blood from one patient. We then kept a small proportion of the PBMCs pre-CTC enrichment to compare immunostaining with staining after CTC enrichment using our different

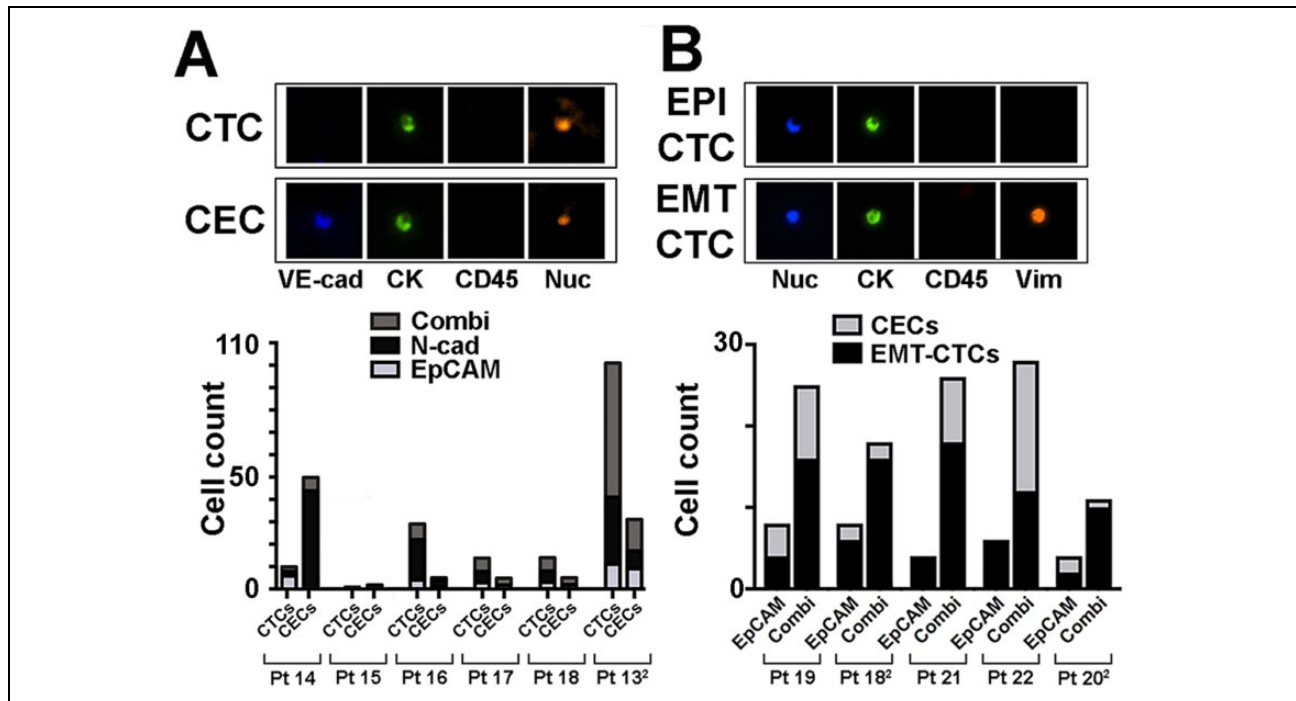


**Figure 3.** CEC and EMT-CTC capture by immunomagnetic isolation (a) top: representative quadruple staining of a CTC (VE-cad<sup>-</sup>, CK<sup>+</sup>, CD45<sup>-</sup>, and Nuc<sup>+</sup>) and CEC staining (VE-cad<sup>+</sup>, CK<sup>+</sup>, CD45<sup>-</sup>, and Nuc<sup>+</sup>). Bottom: ovarian cancer patient cells were isolated by EpCAM, N-cadherin (N-cad), or combined targeting as indicated. The proportion of total CTCs and CECs captured with each isolation strategy is displayed. All counts are presented as cells per 9 ml blood. (b) Top: representative quadruple staining of an epithelial (EPI) and an EMT-phenotype CTCs. Bottom: comparison of EMT-CTC and CECs isolated from advanced ovarian cancer patients by EpCAM or combined EpCAM plus N-cadherin (Combi) targeting. All counts are presented as cells per 9 ml blood. CECs: circulating endothelial cells; EMT: epithelial-to-mesenchymal transition; CTCs: circulating tumor cells; CECs: circulating endothelial cells; EpCAM: epithelial cell adhesion molecule.

isolation strategies. To also evaluate N-cadherin expression in that setting, we combined CD45 with VE-cad probing in the green fluorescent channel. The patient evidently had very low CTC numbers (Online Supplementary Table S3). Thus, not surprisingly, we did not detect any CTC in the pre-enriched sample from 1 ml blood but detected four non-CTCs (Nuc<sup>+</sup>/(CD45, VE-cad)<sup>+</sup>/CK<sup>+</sup>). In total, more non-CTCs were detected in the enriched CTC samples, indicating that the patient had high CEC counts which could be appropriately distinguished from CTCs (Online Supplementary Table S3). However, normalized on the blood volume (8.7 ml) only N-cadherin-alone isolation produced similarly high non-CTC numbers, further evidencing that this enrichment strategy may also enrich potential false positives most effectually (Online Supplementary Table S3). The detected non-CTCs might be CECs, although with some uncertainty, due to CD45 and VE-cad detection in the same fluorescent channel in these experiments. Of note, N-cadherin was detected in some but not all of these cells (Online Supplementary Figure S2).

We set out to demonstrate increased isolation efficiency with our method, and blood collections were not restricted to specific time points throughout treatment. Thus, not unexpectedly, no significant correlation between CTC

numbers and disease parameters was observed (data not shown).

## Discussion

The aim of this study was to establish a method to improve immunomagnetic CTC isolation from ovarian cancer patients by capturing both CTCs with epithelial and mesenchymal phenotype. The EMT-phenotype change is characterized by an E-cadherin-to-N-cadherin switch (reviewed by Lamouille et al.<sup>24</sup>), while expectedly the two epithelial markers EpCAM and E-cadherin are closely co-expressed in our large ovarian cancer cell line cohort. Thus, well-established EpCAM-based CTCs isolation is likely adequate to isolate epithelial cells. As expected, we confirmed increased levels of N-cadherin in our ovarian cancer cell lines with low EpCAM levels, and these flow cytometry data informed our decision to add N-cadherin to our immunomagnetic targeting assay using the Isoflux platform. However, it is worth highlighting that N-cadherin was not expressed on approximately 75% of EpCAM-negative A2780 cells, implying that A2780-like CTCs are likely to remain as poorly detectable with our method as with established EpCAM-based CTC isolation methods.

Notably, A2780 ovarian origin has been questioned previously as genetic clustering puts these cells closer to intestinal or lung cancer cells.<sup>25,29</sup>

Our data show that targeting the EMT marker N-cadherin with a commercially available anti-N-cadherin antibody isolates 2.1-fold more CTCs from advanced ovarian cancer patients than EpCAM-alone-based isolation and 3.0-fold more when used together with EpCAM targeting. Our CTC isolation efficiencies from 80% to 90% of patients are comparable to other ovarian cancer studies that detected CTCs from 14% to 85% of patients dependent on disease stage and CTC detection methods.<sup>4,5</sup> Notably, CTC counts when targeting EpCAM alone were similar to those reported in a recent ovarian cancer study using the Isoflux platform (range 0–1208; median 55).<sup>30</sup> In comparison to EpCAM-alone-targeted CTC isolation, CTC counts were always higher when N-cadherin was targeted alone or in combination with EpCAM, although some co-purification of CECs was observed when including N-cadherin targeting into isolation strategies.

In our study, N-cadherin-alone-based isolation of CTCs always improved on EpCAM-alone-based isolation. Also, the combined targeting always improved on EpCAM-alone targeting; however, the combination strategy was only superior to N-cadherin-alone-based CTC isolation in about half of the samples. We speculate that immunomagnetic beads with different antibodies in the same admixture can cause interference with cell capture if only one of the targeted antigens is predominantly expressed. Thus, an EMT-CTC population predominantly expressing N-cadherin would be expected to be more efficiently isolated with N-cadherin-only targeting than by adding potentially interfering beads coupled to, in the context less relevant, anti-EpCAM antibodies. We, therefore, propose that antibody cocktails used in CTC isolation should be considered with caution, as antibodies that might only aid in exceptional cases to isolate relatively rare cells may interfere in the appropriate isolation of the intended common cell population. Nevertheless, we propose that combining EpCAM with N-cadherin-based ovarian cancer CTC isolation will ultimately be a more successful strategy, particularly if also investigating early-stage patients, who would be expected to have more epithelial CTC phenotypes.

Our data confirm that, similar to size filtration-based CTC enrichment methods, CTC isolation strategies focusing not only on EpCAM expressing CTCs lead to higher total CTC counts.<sup>31,15</sup> However, we confirm that EpCAM-only-based CTC isolation yields purer CTC populations as contamination with false positives is rare in comparison to N-cadherin-based CTC isolation. Our data also confirm, importantly, that CECs are an important cause of false-positive CTC identification and are not distinguished by the common CTC identification (Nuc+/CK+/CD45-). Moreover, CECs not only express N-cadherin but also a number of other markers that have been previously proposed for CTC isolation, such as Epidermal growth factor

receptor (EGFR), vimentin, and fibronectin. With a cell size ranging up to around 10  $\mu\text{m}$ , they may also not be filtered out sufficiently by size exclusion methods of CTC isolation. Our data agree with studies that specifically targeted CECs for isolation, where CEC counts were highly variable in healthy individuals (0–29/ml blood) and tended to be increased in some disease states including cancer (reviewed by Po et al.<sup>28</sup>). Therefore, it is important to account for CECs when using any non-EpCAM-based CTC isolation method. We developed quadruple-stain CTC identification (Nuc+/CK+/CD45-/VE-cad-) that largely diminishes the identification of false-positive CTCs by distinguishing them from co-isolated CECs. Importantly, regardless of whether CECs might make up a varying predominantly smaller proportion of cells in a CTC isolate, parallel samples confirmed that immunomagnetic CTC isolation based on EpCAM plus N-cadherin does isolate more EMT-phenotype CTCs than EpCAM targeting and any CEC can be readily distinguished. This indicates that although CECs can be considerable for a few individuals, when isolating CTCs by other than EpCAM-based methods, they play mostly a minor role especially if a study only analyses CTC numbers.

Our study was aimed to improve immunomagnetic CTC isolation by also targeting EMT-CTCs, and we confirmed our isolation strategy in predominantly advanced disease ovarian cancer patients. Our patient recruitment did not require liquid biopsies at specific times during a patient's disease progression or with regard to timing before and after treatment cycles. In our small heterogeneous cohort used for method validation, we, therefore, did not observe any obvious correlation of CTC counts with disease stage or outcomes. We did, however, capture a larger number of CTCs in a higher proportion of advanced ovarian cancer patients by combined targeting of EpCAM and N-cadherin for immunomagnetic isolation. Therefore, our data also support the notion that ovarian cancer CTCs are more heterogeneous with regard to EMT status, which agrees with the findings that emerging EMT-phenotype CTCs might be associated with response to therapy.<sup>19</sup>

In conclusion, we established a combined EpCAM and N-cadherin immunomagnetic targeting strategy to improve on the overall CTC isolation. We suggest that non-EpCAM-based CTC isolation methods should employ a quadruple staining method to avoid false positives. The significance of detecting more and a wider range of CTC phenotypes is that they are more likely to accurately represent the biology of a patient's ovarian cancer at that point in time, thus improving their value as potential tumor biomarkers. Finally, our combined antibody targeting approach may also be useful in improving CTC capture in other cancer types.

#### Acknowledgements

We thank the members of the Gynaecological Oncology Biobank Westmead (member of the Australasian Biospecimen Network-



Oncology group, funded by the Australian National Health and Medical Research Council, Enabling Grants ID 310670 & ID 628903 and the Cancer Institute NSW Grants ID 12/RIG/1-17 & 15/RIG/1-16) for patient recruitment. WME-099 cells were kindly provided by Professor Graham Mann. Human ethics approval, HREC/13/LPOOL/158, was obtained and managed by the CONCERT Biobank.

### Declaration of Conflicting Interests

The author/s declared no conflicts of interest with respect to the research, authorship, and/or publication of this article.

### Funding

The authors disclosed receipt of the following financial support for the research, authorship, and/or publication of this article: JP and DL are recipients of Rotary Health Australia and Ingham Research Director's PhD Scholarships, respectively. PdS<sup>1</sup>, TMB<sup>1</sup>, AdeF<sup>2</sup>, and PRH<sup>2</sup> are supported by the Cancer Institute New South Wales through; <sup>1</sup>the Centre for Oncology Education and Research Translation (CONCERT), and <sup>2</sup>the Sydney-West Translational Cancer Research Centre. AdeF was also funded by the University of Sydney.

### Supplemental material

Supplementary material for this article is available online.

### References

- Kim A, Ueda Y, Naka T, et al. Therapeutic strategies in epithelial ovarian cancer. *J Exp Clin Cancer Res* 2012; 31: 14.
- Matsuo K, Lin YG, Roman LD, et al. Overcoming platinum resistance in ovarian carcinoma. *Expert Opin Investig Drugs* 2010; 19(11): 1339–1354.
- Caixeiro NJ, Kienzle N, Lim SH, et al. Circulating tumour cells—a bona fide cause of metastatic cancer. *Cancer Metastasis Rev* 2014; 33(2–3): 747–756.
- Poveda A, Kaye SB, McCormack R, et al. Circulating tumor cells predict progression free survival and overall survival in patients with relapsed/recurrent advanced ovarian cancer. *Gynecol Oncol* 2011; 122(3): 567–572.
- Pearl ML, Dong H, Tulley S, et al. Treatment monitoring of patients with epithelial ovarian cancer using invasive circulating tumor cells (iCTCs). *Gynecol Oncol* 2015; 137(2): 229–238.
- Romero-Laorden N, Olmos D, Fehm T, et al. Circulating and disseminated tumor cells in ovarian cancer: a systematic review. *Gynecol Oncol* 2014; 133(3): 632–639.
- Cui L, Kwong J, and Wang CC. Prognostic value of circulating tumor cells and disseminated tumor cells in patients with ovarian cancer: a systematic review and meta-analysis. *J Ovarian Res* 2015; 8(1): 38.
- Zhou Y, Bian B, Yuan X, et al. Prognostic value of circulating tumor cells in ovarian cancer: a meta-analysis. *PloS One* 2015; 10(6): e0130873.
- Zeng L, Liang X, Liu Q, et al. The predictive value of circulating tumor cells in ovarian cancer: a meta analysis. *Int J Gynecol Cancer* 2017; 27(6): 1109–1117.
- Chebouti I, Kuhlmann JD, Buderath P, et al. ERCC1-expressing circulating tumor cells as a potential diagnostic tool for monitoring response to platinum-based chemotherapy and for predicting post-therapeutic outcome of ovarian cancer. *Oncotarget* 2017; 8(15): 24303–24313.
- Pearl ML, Dong H, Zhao Q, et al. iCTC Drug Resistance (CDR) testing ex vivo for evaluation of available therapies to treat patients with epithelial ovarian cancer. *Gynecol Oncol* 2017; 147: 426–432.
- Lee M, Kim EJ, Cho Y, et al. Predictive value of circulating tumor cells (CTCs) captured by microfluidic device in patients with epithelial ovarian cancer. *Gynecol Oncol* 2017; 145(2): 361–365.
- Pradeep S, Kim SW, Wu SY, et al. Hematogenous metastasis of ovarian cancer: rethinking mode of spread. *Cancer Cell* 2014; 26(1): 77–91.
- Van Berckelaer C, Brouwers AJ, Peeters DJ, et al. Current and future role of circulating tumor cells in patients with epithelial ovarian cancer. *Eur J Surg Oncol* 2016; 42(12): 1772–1779.
- Punnoose EA, Atwal SK, Spoerke JM, et al. Molecular biomarker analyses using circulating tumor cells. *PloS One* 2010; 5(9): e12517.
- Gorges TM, Tinhofer I, Drosch M, et al. Circulating tumour cells escape from EpCAM-based detection due to epithelial-to-mesenchymal transition. *BMC Cancer* 2012; 12: 178.
- Stimpfl M, Schmid BC, Schiebel I, et al. Expression of mucins and cytokeratins in ovarian cancer cell lines. *Cancer Lett* 1999; 145(1–2): 133–141.
- Tsai JH and Yang J. Epithelial-mesenchymal plasticity in carcinoma metastasis. *Genes Dev* 2013; 27(20): 2192–2206.
- Chebouti I, Kasimir-Bauer S, Buderath P, et al. EMT-like circulating tumor cells in ovarian cancer patients are enriched by platinum-based chemotherapy. *Oncotarget* 2017; 8(30): 48820–48831.
- Haslehurst AM, Koti M, Dharsee M, et al. EMT transcription factors snail and slug directly contribute to cisplatin resistance in ovarian cancer. *BMC Cancer* 2012; 12: 91.
- Marchini S, Fruscio R, Clivio L, et al. Resistance to platinum-based chemotherapy is associated with epithelial to mesenchymal transition in epithelial ovarian cancer. *Eur J Cancer* 2013; 49(2): 520–530.
- Tohill RW, Tinker AV, George J, et al. Novel molecular subtypes of serous and endometrioid ovarian cancer linked to clinical outcome. *Clin Cancer Res* 2008; 14(16): 5198–5208.
- Miow QH, Tan TZ, Ye J, et al. Epithelial-mesenchymal status renders differential responses to cisplatin in ovarian cancer. *Oncogene* 2015; 34(15): 1899–1907.
- Lamouille S, Xu J, and Derynck R. Molecular mechanisms of epithelial-mesenchymal transition. *Nat Rev Mol Cell Biol* 2014; 15(3): 178–196.
- Quattrocchi L, Green AR, Martin S, et al. The cadherin switch in ovarian high-grade serous carcinoma is associated with disease progression. *Virch Arch* 2011; 459(1): 21–29.

26. Davidson B, Trope CG, and Reich R. Epithelial-mesenchymal transition in ovarian carcinoma. *Front Oncol* 2012; 2: 33.
27. Chung VY, Tan TZ, Tan M, et al. GRHL2-miR-200-ZEB1 maintains the epithelial status of ovarian cancer through transcriptional regulation and histone modification. *Sci Rep* 2016; 6: 19943.
28. Po JW, Lynch D, de Souza P, et al. Importance and detection of epithelial-to-mesenchymal transition (EMT) phenotype in CTCs. In: Xu K (ed) *Tumor metastasis*. Nigeria: InTech, 2016, pp. 241–256.
29. Domcke S, Sinha R, Levine DA, et al. Evaluating cell lines as tumour models by comparison of genomic profiles. *Nat Commun* 2013; 4: 2126.
30. Rao Q, Zhang Q, Zheng C, et al. Detection of circulating tumour cells in patients with epithelial ovarian cancer by a microfluidic system. *Int J Clin Exp Pathol* 2017; 10: 9699–9706.
31. Krebs MG, Hou JM, Sloane R, et al. Analysis of circulating tumor cells in patients with non-small cell lung cancer using epithelial marker-dependent and -independent approaches. *J Thorac Oncol* 2012; 7(2): 306–315.